Mechanics of Advanced Composite Structures

Semnan University

journal homepage: http://MACS.journals.semnan.ac.ir

Semi Analytical Transient Dynamic Analysis of Composite Adhesive Single-lap Joints

E. Selahi*

Department of Mechanical Engineering, Marvdasht Branch Islamic Azad University, 73711-13119, Marvdasht, Iran

KEYWORDS

Adhesive joint
Adherend
Transient dynamic
Laminated Composite
Peel and shear stresses

ABSTRACT

A novel semi analytical method is developed for transient analysis of single-lap adhesive joints with laminated composite adherends subjected to dynamical loads. The presented approach has the capability of choosing arbitrary loadings and boundary conditions. In this model, adherends are assumed to be orthotropic plates that pursuant to the classical lamination theory. Stacking sequences can be either symmetric or asymmetric. The adhesive layer is homogenous and isotropic material and modelled as continuously distributed normal and shear springs. By applying constitutive, kinematics, and equations of motions, sets of governing differential equations for each inside and outside of overlap zones are acquired. By solving these equations, the time dependent shear and peel stresses in adhesive layer as well as deflections, stress resultants, and moment resultants in the adherends are computed. The developed results are successfully compared with the experimental research presented in available literates. It is observed that the time variations of adhesive peel and shear stress diagrams are asymmetric for the case of symmetric applied load with high variation rate. Moreover, it is reported that although the magnitude of applied transverse shear force is reduced to 10% of applied axial force, however a significant increase of 40% in the maximum peel stress attained.

1. Introduction

Joint technology is applied in order to transmit structural loads from one component to another. Conventional joining methods in composite structures are: adhesive joints and bolted joints. Advantages of adhesive joints with respect to bolted joints are as follow:

- Relatively uniform stress distribution
- Weight reduction (especially in narrow joints)
- Vibration damping capability
- The capability of joining and sealing simultaneously
- Ease of fabrication process
- Reducing production cost

Presebtible researches have investigated the behaviour of adhesive joints at the condition of static equilibrium.

The first research in modeling of adhesive joints was employed by Volkersen [1]. He analysed a single-lap adhesive joint; in this model, the adhesive layer was approximated by continuous shear springs. The weakness of this model is the lack of contemplating bending moment caused by the presence of eccentricity in the loading path. Later, this model was modified by Goland et al. [2]. They modelled the adhesive layer in terms of continuous shear and normal springs.

Hart-Smith [3-5], presented some mathematical relations to examine the structural behaviour of various types of adhesively bonded joints with metallic adherends. Mortensen and Thomsen [6] explored single-lap adhesive joint with orthotropic sdherends. In this model adhesive layer is continuously linear shear and tension/compression springs.

Selahi et al. [7-12] presented mathematical relations for different geometry of adhesively bonded composite joints, with linear and non-linear behaviour. Benchiha and Madani [13] employed the finite element method (FEM) in order to inspect the distribution of adhesive shear stresses in the single-lap joint with two aluminium 2024-T3 adherends, with and without defects.

Few published works have revolved around the dynamical behaviour of the adhesive joints with laminated composite adherends, and most of them are based on objective researches. The

* Corresponding author. Tel.: +98-71-43112201
E-mail address: selahi@miau.ac.ir

DOI: 10.22075/MACS.2019.16036.1161
Received 2018-09-27; Received in revised form 2019-07-03; Accepted 2019-10-27

most important of these researches are as follows:

Radice and Vinson [14], presented a solution methodology for quasi dynamic modelling of composite adhesive joints. Wu et al. [15], inspected the crashworthiness of epoxy adhesively bonded joints for carbon fibre reinforced composite panels under transverse loading experimentally.

Hazimeh et al. [16], employed three-dimensional finite element (FE) analysis in order to inquire about the behaviour of composite double lap adhesive joints subjected to dynamic in-plane impact loadings. Araújo et al. [17] developed FE models with cohesive elements in ABAQUS software to examinethe behaviour of composite single lap adhesive joints under quasi-static and impact loadings. Dynamic strength of composite adhesive joints with similar and dissimilar adherends are investigated experimentally by He and Ge [18].

Recently Argoud et al. [19] presented an experimental study on the adhesively bonded joints with fibre reinforced thermoplastic composite adherends. They explored the effect of load orientation, temperature, loading speed and adhesive thickness on stiffness, strength and energy absorption of the joints. Sassi et al. [20, 21] surveyed the behaviour of in-plane and out-of-plane dynamic response of composite adhesive joints under dynamic compression at high strain rate tests.

Despite the fact that in most cases, joints are subjected to dynamical or quasi dynamical loadings. On that account, the aforementioned review motivated us to present an efficient semi analytical method for transient analysing of composite adhesive joint subjected to in-plane dynamic loadings.

2. Theoretical development

Transient dynamic mathematical modelling of adhesive joints with laminated composite adherends were acquired by adopting sets of restrictive assumptions for description the behaviour of bonded joints. Pursuant to these assumptions, constitutive and kinematics relations for each of the adherends and constitutive relations for adhesive layer were obtained. By combining these relations and equations, governing equations in the form of a system of partial differential equations, for each zone (inside and outside of overlap zone) were acquired. Assumptions for the adherends, adhesive layers, loading and boundary conditions are as follows:

- Adherends:
  - ✓ Adherends were modelled as wide beams.
  - ✓ Adherends are orthotropic laminates that obeyed with the time dependent classical lamination theory.
  - ✓ The laminates have linear elastic behaviour.
- Adhesive layer:
  - ✓ The adhesive layer was assumed to behave as homogenous, isotropic and elastic materials.
  - ✓ The adhesive layer was modelled as continuously distributed linear shear and tension\compression springs.

The adhesive joint consists of two parts of internal and external zones. It is noteworthy to mention that the connection is made in the internal region. Therefore, the governing equations in the inside of overlap zone are much more complicated compare to the governing equations in the outside of overlap zones. The common adhesive lap joints are single-lap, double-lap, double-strap, and single-scarf. Here for the sake of brevity, the only single-lap adhesive joint was inspected, although the governing equations can be generalized easily to the other types of adhesive joints. Fig. 1 shows a single-lap adhesive joint subjected to different dynamical loadings at the free ends as follows:

N_x : Extensional resultant force

Q_x : Shear resultant force

M_x : Bending resultant force.

2.1. Mathematical modelling in the inside of overlap zone

Here adherends are orthotropic laminates with either symmetric or asymmetric stacking sequences. In the modelling of adherends as wide beams, the transverse displacements are ignored. Also, in the classical lamination theory, ε_z is assumed to be zero so that displacement components are only functions of time (t) and axial coordinate (x), as shown in Eqs. (1) and (2).

$$u_0^i = u_0^i(x,t) \tag{1}$$

$$w^i = w^i(x,t) \tag{2}$$

where: u_0^i is a mid-plane displacement in the x directions and w^i is a through thickness displacement component in i^{th} adherends. Here i=1 and 2.

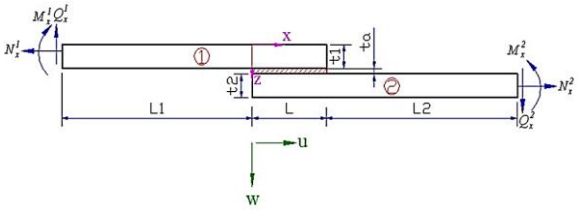

Fig. 1. Single lap adhesive joint

Consequently, the time dependent classical lamination theory for wide beams is simplified as Eqs. (3) and (4):

$$N_x^i(x,t) = A_{11}^i u_{0,x}^i(x,t) - B_{11}^i w_{,xx}^i(x,t) \quad (3)$$

$$M_x^i(x,t) = B_{11}^i u_{0,x}^i(x,t) - D_{11}^i w_{,xx}^j(x,t) \quad (4)$$

Kinematic relations for adherends are as follows:

$$u^i(x,t) = u_0^i(x,t) - z\,\beta_x^i(x,t) \quad (5)$$

$$w_{,x}^i(x,t) = \beta_x^i(x,t) \quad (6)$$

where u^i is axial displacement. According Eqs. (3), (4) and (6), Eqs. (7) and (8) are derived.

$$u_{0,x}^i(x,t) = \frac{D_{11}^{\ i} N_x^i(x,t) - B_{11}^i M_x^i(x,t)}{A_{11}^i D_{11}^i - B_{11}^{i\ 2}} \quad (7)$$

$$\beta_{,x}^i(x,t) = \frac{B_{11}^{\ i} N_x^i(x,t) - A_{11}^i M_x^i(x,t)}{A_{11}^i D_{11}^i - B_{11}^{i\ 2}} \quad (8)$$

For the case of laminated composite adherends with symmetric stacking sequences, the Eqs. (7) and (8) are simplified as follows:

$$u_{0,x}^i(x,t) = \frac{1}{A_{11}^i} N_x^i(x,t) \quad (9)$$

$$\beta_{,x}^i(x,t) = \frac{-1}{D_{11}^i} M_x^i(x,t) \quad (10)$$

where A, B, and D are extensional, coupling, and bending stiffness matrices, respectively, which are defined by the Eqs. (11)-(13).

$$A_{ij} = \sum_{k=1}^{n} (\overline{Q}_{ij})_k (z_k - z_{k-1}) \quad (11)$$

$$B_{ij} = \frac{1}{2}\sum_{k=1}^{n} (\overline{Q}_{ij})_k (z_k^2 - z_{k-1}^2) \quad (12)$$

$$D_{ij} = \frac{1}{3}\sum_{k=1}^{n} (\overline{Q}_{ij})_k (z_k^3 - z_{k-1}^3) \quad (13)$$

In this model the adhesive layer was modelled as continuously distributed linear shear and tension/compression springs. The developed shear and peel stresses in the adhesive layer were computed by Eqs. (14) and (15).

$$\sigma(x,t) = E_a \varepsilon(x,t) = \frac{E_a}{t_a}\left[w^i(x,t) - w^j(x,t)\right] \quad (14)$$

$$\tau(x,t) = G_a \gamma(x,t) = \frac{G_a}{t_a}\left[u_0^i(x,t) + \frac{t_i}{2}\beta^i(x,t) - u_0^j(x,t) + \frac{t_j}{2}\beta^j(x,t)\right] \quad (15)$$

where, σ, τ, ε and γ denote, peel stress, shear stress, peel strain and shear strain in the adhesive layer respectively. t_a is the thickness of adhesive layer, E_a and G_a are moduli of elasticity and shear modulus, respectively, and $i \neq j$ are adherend numbers.

Each element in the inside of the overlap zone included an element of adherend with half thickness of adhesive layer. Fig. 2 illustrated the forces applied in each element in the inside of overlap zone for single-lap adhesive joint.

Pursuant to Fig. 2, the equations of motion in the inside of overlap zone are determined as follows:

$$\begin{aligned}
&N_{x,x}^1(x,t) + \tau(x,t) = I_1^1 \frac{\partial^2 u_0^1(x,t)}{\partial t^2} \\
&Q_{x,x}^1(x,t) + \sigma(x,t) = I_1^1 \frac{\partial^2 w^1(x,t)}{\partial t^2} \\
&M_{x,x}^1(x,t) - Q_x^1(x,t) + \tau(x,t)\frac{t_1 + t_a}{2} = I_3^1 \frac{\partial^2 \beta^1(x,t)}{\partial t^2} \\
&N_{x,x}^2(x,t) - \tau(x,t) = I_1^2 \frac{\partial^2 u_0^2(x,t)}{\partial t^2} \\
&Q_{x,x}^2(x,t) - \sigma(x,t) = I_1^2 \frac{\partial^2 w^2(x,t)}{\partial t^2} \\
&M_{x,x}^2(x,t) - Q_x^2(x,t) + \tau(x,t)\frac{t_2 + t_a}{2} = I_3^2 \frac{\partial^2 \beta^2(x,t)}{\partial t^2}
\end{aligned} \quad (16)$$

Inertias I_1 and I_3 are defined by Eqs. (17) and (18):

$$I_1^j = \sum_{i=1}^{N} \rho_i (z_k - z_{k-1}) \quad (17)$$

$$I_3^j = \frac{1}{3}\sum_{i=1}^{N} \rho_i (z_k^3 - z_{k-1}^3) \quad (18)$$

By combining constitutive and kinematic relations in adherends and adhesive layers with equations of motions in the inside of overlap zones, the governing equations in the inside of overlap region are derived. The governing equations are a system of fully coupled partial differential equations with general form of:

$$\frac{d}{dx}\{X(x,t)\} + [A]\{X(x,t)\} = [B]\frac{d^2}{dt^2}\{X(x,t)\}.$$

Here, X is an unknown vector with 12 components, and A and B are constant coefficient matrices with 12 rows and columns. The detailed governing equations of single-lap adhesive joints subjected to dynamical loads were depicted in Eq. (19).

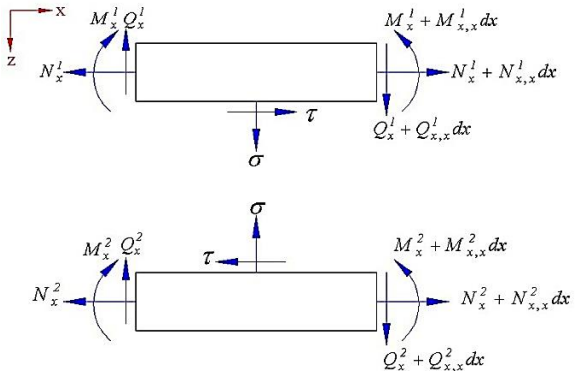

Fig. 2. A schematics of elements in the inside of overlap zone for single lap joint

$$
\begin{cases}
u^1_{0,x}(x,t)-\dfrac{D^1_{11}N^1_x(x,t)-B^1_{11}M^1_x(x,t)}{A^1_{11}D^1_{11}-B^{1\,2}_{11}}=0 \xrightarrow{Symmetrical\ StackingSequence} u^1_{0,x}(x,t)-\dfrac{1}{A^1_{11}}N^1_x(x,t)=0 \\
\beta^1_{,x}(x,t)-\dfrac{B^1_{11}N^1_x(x,t)-A^1_{11}M^1_x(x,t)}{A^1_{11}D^1_{11}-B^{1\,2}_{11}}=0 \xrightarrow{Symmetrical\ StackingSequence} \beta^1_{,x}(x,t)+\dfrac{1}{D^1_{11}}M^1_x(x,t)=0 \\
w^1_{,x}(x,t)-\beta^1(x,t)=0 \\
N^1_{x,x}(x,t)-\dfrac{G_a}{t_a}\left\{u^1_0(x,t)-\dfrac{t_1}{2}\beta^1(x,t)-u^2_0(x,t)-\dfrac{t_2}{2}\beta^2(x,t)\right\}=I^1_1\dfrac{\partial^2u^1_0(x,t)}{\partial t^2} \\
Q^1_{x,x}(x,t)-\dfrac{E_a}{t_a}\left\{w^1(x,t)-w^2(x,t)\right\}=I^1_1\dfrac{\partial^2w^1(x,t)}{\partial t^2} \\
M^1_{x,x}(x,t)-Q^1_x(x,t)-\dfrac{G_a}{t_a}\left\{u^1_0(x,t)-\dfrac{t_1}{2}\beta^1(x,t)-u^2_0(x,t)-\dfrac{t_2}{2}\beta^2(x,t)\right\}\dfrac{t_1+t_a}{2}=I^1_3\dfrac{\partial^2\beta^1(x,t)}{\partial t^2} \\
u^2_{0,x}(x,t)-\dfrac{D^2_{11}N^2_x(x,t)-B^2_{11}M^2_x(x,t)}{A^2_{11}D^2_{11}-B^{2\,2}_{11}}=0 \xrightarrow{Symmetrical\ StackingSequence} u^2_{0,x}(x,t)-\dfrac{1}{A^2_{11}}N^2_x(x,t)=0 \\
\beta^2_{,x}(x,t)-\dfrac{B^2_{11}N^2_x(x,t)-A^2_{11}M^2_x(x,t)}{A^2_{11}D^2_{11}-B^{2\,2}_{11}}=0 \xrightarrow{Symmetrical\ StackingSequence} \beta^2_{,x}(x,t)+\dfrac{1}{D^2_{11}}M^2_x(x,t)=0 \\
w^2_{,x}(x,t)-\beta^2(x,t)=0 \\
N^2_{x,x}(x,t)-\dfrac{G_a}{t_a}\left\{-u^1_0(x,t)+\dfrac{t_1}{2}\beta^1(x,t)+u^2_0(x,t)+\dfrac{t_2}{2}\beta^2(x,t)\right\}=I^2_1\dfrac{\partial^2u^2_0(x,t)}{\partial t^2} \\
Q^2_{x,x}(x,t)-\dfrac{E_a}{t_a}\left\{-w^1(x,t)+w^2(x,t)\right\}=I^2_1\dfrac{\partial^2w^2(x,t)}{\partial t^2} \\
M^2_{x,x}(x,t)-Q^2_x(x,t)-\dfrac{G_a}{t_a}\left\{u^1_0(x,t)-\dfrac{t_1}{2}\beta^1(x,t)-u^2_0(x,t)-\dfrac{t_2}{2}\beta^2(x,t)\right\}\dfrac{t_2+t_a}{2}=I^2_3\dfrac{\partial^2\beta^2(x,t)}{\partial t^2}
\end{cases}
\tag{19}
$$

Due to the separability of the partial differential system of equations (19), the governing equations have the solutions in the general form of:

$$
\begin{aligned}
&\{U(x,t)\}=\{X(x)\}.\{T(t)\}\rightarrow \\
&\frac{\{X'\}+[A]\{X\}}{\{X\}}=\frac{[B]\{\ddot{T}\}}{\{T\}}=[\lambda]
\end{aligned}
\tag{20}
$$

where

$$
\begin{cases}
\{X\}=\{X_0\}e^{[\lambda-A]x} \\
\{T\}=\{C_1\}e^{[\lambda/B]t}+\{C_2\}e^{-[\lambda/B]t}
\end{cases}
\tag{21}
$$

Vectors C_1, C_2, and X_0 are determined by considering the initial and boundary conditions respectively.

2.2. Mathematical modelling in outside of overlap zone

In the outside of the overlap zone, the kinematics and constitutive equations are similar to the inside of overlap zone. Moreover, in this region, as a result of lack of adhesive layer, peel and shear stress in the adhesive layer are not appear in the equations of motion. In Fig. 3, the forces applied in each element in the outside of overlap zone were indicated.

Therefore, the equations of motion in the outside of the overlap zone were computed as:

$$
\begin{aligned}
&N^j_{x,x}(x,t)=I^j_1\frac{\partial^2u^j_0(x,t)}{\partial t^2} \\
&Q^j_{x,x}(x,t)=I^j_1\frac{\partial^2w^j(x,t)}{\partial t^2} \\
&M^j_{x,x}(x,t)-Q^j_x(x,t)=I^j_3\frac{\partial^2\beta^j(x,t)}{\partial t^2}
\end{aligned}
\tag{22}
$$

It is noticeable that the bending resultant force M_x that leads to rotation of adhesive joints can be caused by applying bending moment and transverse shear force as well as the axial force due to eccentricity in the geometry of single-lap adhesive joint. All of these factors are deliberated in the formulations of M_x.

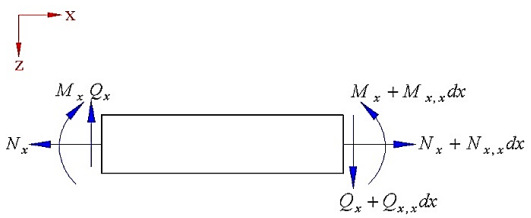

Fig. 3. A schematics of elements in the outside of overlap zone

By combining constitutive and kinematic relations with equations of motions in the outside of overlap zones, the governing equations in each outside of overlap zones are computed. Here the governing equations are a system of partial differential equations as well that depicted as Eq. (23).

$$\begin{cases} u^1_{0,x}(x,t) - \dfrac{1}{A^1_{11}} N^1_x(x,t) = 0 \\ \beta^1_{,x}(x,t) + \dfrac{1}{D^1_{11}} M^1_x(x,t) = 0 \\ w^1_{,x}(x,t) - \beta^1(x,t) = 0 \\ N^j_{x,x}(x,t) = I^j_1 \dfrac{\partial^2 u^j_0(x,t)}{\partial t^2} \\ Q^j_{x,x}(x,t) = I^j_1 \dfrac{\partial^2 w^j(x,t)}{\partial t^2} \\ M^j_{x,x}(x,t) - Q^j_x(x,t) = I^j_3 \dfrac{\partial^2 \beta^j(x,t)}{\partial t^2} \end{cases} \quad (23)$$

3. Results and discussions

3.1. Validation

In order to manifest the validity of the presented transient dynamic modelling method, the time dependent axial displacement variation of a composite single-lap adhesive joint under dynamic axial load is compared with the experimental results presented in Ref. [19].

Adherends are made of fiberglass fabric with polyamide resin, and the adhesive layer is sikaflex. Table 1 listed the geometrical and material properties of the adherends and adhesive layer. Here adherends have orthotropic behaviour, and adhesive layer has isotropic behaviour.

The bonded joint specimen is subjected to dynamic uni-axial tension with a loading speed of 0.5 m/s. In Fig. 4, the results of presented mathematical modelling are compared with experimental dynamic test results of three specimens, mentioned in Ref. [19]. It can be observed that a good agreement is achieved between the results of the aforementioned mathematical method and the experimental results displayed in Ref. [19].

3.2. Definition of adhesive joint

A single-lap adhesive joint with fixed boundary conditions on one side and free boundary condition on the other side is deliberated. The geometry and dimensions of the specimen illustrated in Fig. 5 and referred to the standard ASTM D1002. Here two cases of time dependent loading conditions were contemplated. In the first case, a dynamic extensional resultant force is defined as Eq. (24) and in the second case a dynamic shear resultant force as defined in Eq. (25), were applied at the free end in the time interval of 0 to 1 sec., as portrayed in Fig. 6.

$$N_x = 4\times10^4 (t - t^2) \ \text{N/m} \quad (24)$$

$$Q_x = 4000(t - t^2) \quad \text{N/m} \quad (25)$$

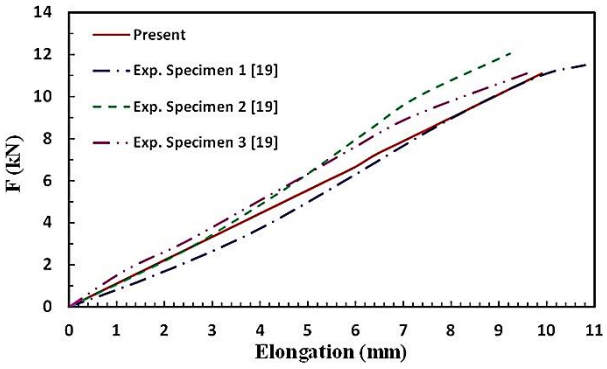

Fig. 4. Comparison of loading displacement curve calculated by presented mathematical modeling with experimental results

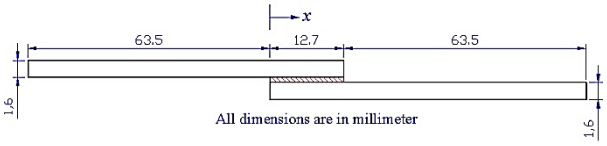

Fig. 5. Dimensions of composite adhesive single lap joint in ASTM D1002

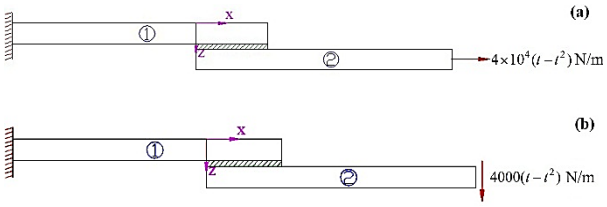

Fig. 6. Single-lap adhesive joint subjected to dynamic a) axial and b) shear loadings

Table 1. Geometrical and material properties of adherends and adhesive layer [19]

Material	Material properties				Geometrical properties		
	Density (kg/m3)	Longitudinal Modulus (MPa)	Transverse Modulus (MPa)	Shear Modulus (MPa)	Length (mm)	Width (mm)	Thickness (mm)
Glass fibre fabric-Polyamide	1187	26000	24000	3370	70	36	2
Sikaflex adhesive	1200	6	6	2	60	20	3

Adherends were made of 8 layers of uni-directional fiberglass/epoxy with symmetric stacking sequences of: $[0^\circ, 45^\circ, -45^\circ, 90^\circ]_{Sym}$. The thickness of each layer is 0.2 mm. The adhesive layer is epoxy AY103 (Ciba Geigy). In Table 2, material properties of the adherend laminas and epoxy adhesive layer are presented.

3.3. Dynamic results

In order to inspect the dynamic behaviour of the introduced adhesive joint, at first, the governing equations in the left outside of overlap zone are solved by Eq. set (23) and by deliberating initial conditions and boundary conditions in $x = -63.5$ mm. Consequently, through solving governing equations in the inside of overlap zone (Eq. 19) and applying initial and boundary conditions in $x = 0$ and $x = 12.7$ mm, the magnitudes of $u_0^1, \beta^1, w^1, Q^1, N^1, M^1, u_0^2, \beta^2, w^2, N^2, Q^2$ and M^2 in each time and each point of inside overlap zone are computed.

In the 3rd step, the adhesive peel and shear stresses were determined applied Eqs. (13) and (14) respectively. At last, the governing equations in the right outside of the overlap zone are solved. Fig. 7 illustrated the time histories and longitudinal variations of deflections, stress resultants and moment resultants in the upper adherend at the outside of overlap zone subjected to dynamic axial load with Eq. (24).

The results of Fig. 7 indicates a perceptible large through thickness displacement components w^1 and w^2. This is a result of the eccentricity in the geometry of a single-lap adhesive joint that generates significant bending moment in the adherends.

Time variation diagrams of shear and peel stresses in the adhesive layer at the beginning (x=0), mid length (x=6.35 mm), and end (x=12.7 mm) of bonded joints subjected to introduced dynamic axial and shear loads were shown in Figs. 8 and 9, respectively.

Furthermore, the acquired results were compared with similar FE analysis applying ANSYS software. The FE models are generated by using 2D solid elements, and each element consists of 8 nodes.

The loading path eccentricity in the single-lap joint generates considerable bending moment that introduced high peel stress in the adhesive layer. The maximum both shear and peel stresses in the adhesive layer occur at the edges of overlap zone (x=0). This is due to high bending moment in the upper adherend generates at this position.

The stress diagrams of Figs. 8 and 9 indicated that, although the transient force is symmetrical in time, due to the high rate of force variation, the stress diagrams are asymmetric.On that account, exactly at the end of the loading time, the amount of applied force is zero; however the magnitude of shear and peel stresses are not zero. This is due to non-zero strain at end of the loading time.

The magnitude of applying axial force is 10 times of the shear force. But comparing the diagrams of Figs. 8 and 9 displays more peel stress that produced in the adhesive layer of bonded joint under shear force. This is due to having long adherends that generate significant bending moments. Generally, in the case of dynamic axial load, shear stress is the dominant stress in the adhesive layer, while peel stress is dominant stress in the adhesive layer of bonded joints subjected to dynamical transverse shear and bending loads.

At last, the adhesive shear and peel stresses acquired from the presented mathematical modelling are highly consistent with the FE simulation results. Thus, the maximum difference between these two methods is 11%, which is related to the shear stress of the adhesive layer in the joint subjected to dynamic shear load.

4. Conclusions

As a result of the essentialness of the dynamic analysis of adhesive joints, a semi analytical method is presented for transient analysis of adhesive single-lap joints with laminated composite adherends subjected to dynamical loads. In this paper, adhesive layer was assumed to behave as homogenous, isotropic and elastic materials and modelled as continuously distributed shear and tension/compression springs. Adherends are linear elastic and orthotropic laminates that obeyed with the time dependent classical lamination theory and made of arbitrary stacking sequences.

Pursuant to these assumptions, constitutive and kinematics relations for each of the adherends and constitutive relations for adhesive layer were obtained. Then equations of motions for each element in the inside and outside of overlap zone were derived. By combining these relations and equations, governing equations in the form of a system of coupled partial differential equations for each zone (inside and outside of overlap zone) are obtained. By solving these equations, the time dependent shear and peel stresses in adhesive layer as well as deflections, stress resultants, and moment resultants in the adherends were determined.

The presented solution method was successfully compared with the experimental dynamic test results of three adhesive joint specimens displayed in available literates. The developed results reveal that the maximum both shear and peel stresses in the adhesive layer occur at the edges of overlap zone (x=0).

Table 2. Material properties of the adherend laminas and epoxy adhesive layer

Part	Material	Properties
Adherend	Fiberglass/Epoxy	E_1=36.8 GPa, E_2=E_3=8.27 GPa, G_{12}= G_{13}=4.14 GPa, G_{23}=3 GPa
		ν_{12}= ν_{13}=0.26, ν_{23}=0.38, ρ=1660 kg/m^3, t=0.2 mm
Adhesive	Epoxy AY103 (Ciba Geigy)	E_a=2.8 GPa, ν_a=0.4, t_a=0.4 mm

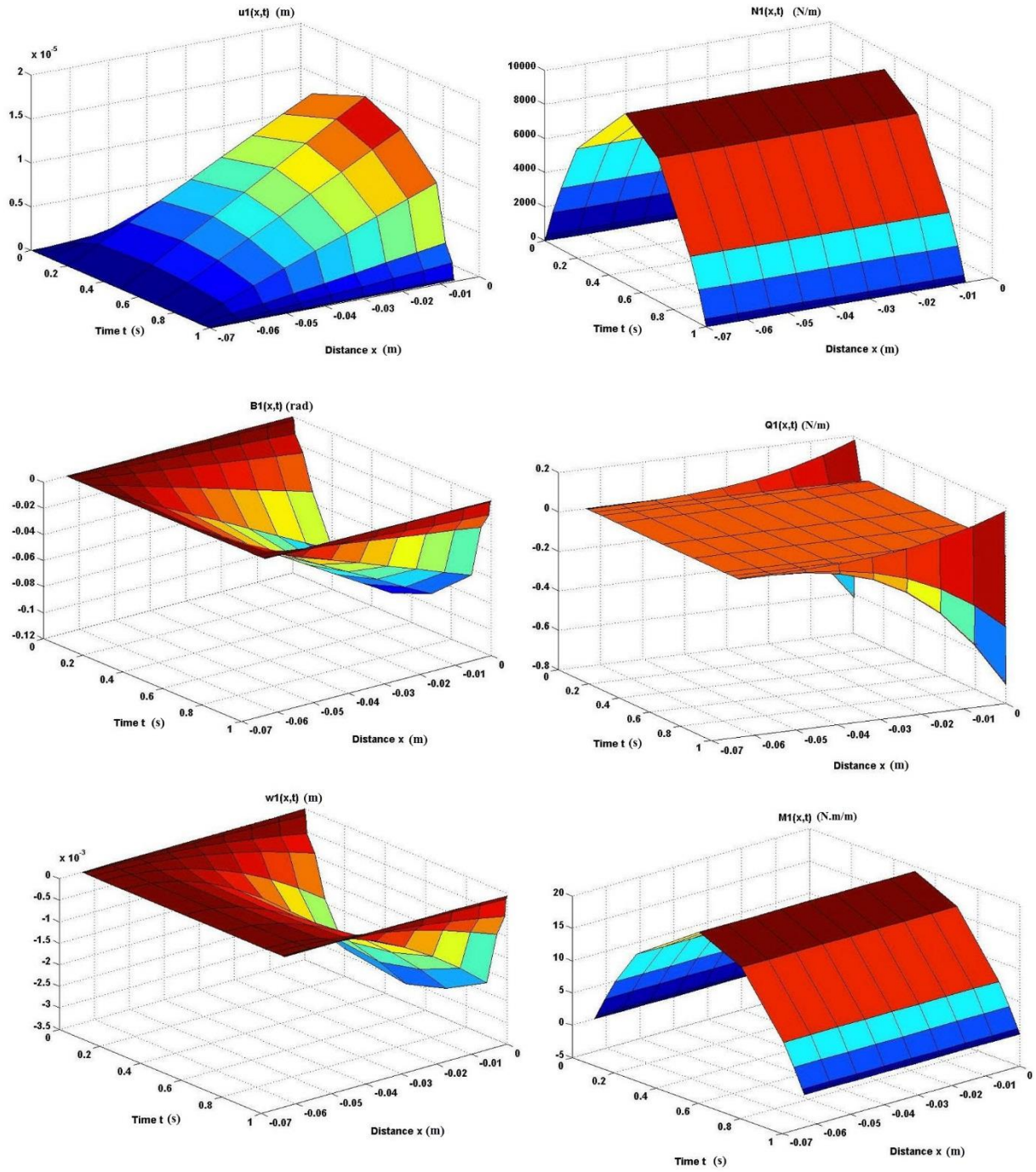

Fig. 7. Time histories and longitudinal variations of deflections, stress resultants and moment resultants in the outside of overlap zone

Moreover, as a result of the high rate of force variation, the stress diagrams are asymmetric for the case of symmetric loading. Therefore, at the end of the loading, the magnitude of the applied force is zero, but non-zero stress components are achieved. At last, when the specimen is subjected to dynamic axial load, shear stress is the dominant stress in the adhesive layer, while peel stress is dominant stress in the adhesive layer of bonded joints subjected to dynamic transverse shear and bending loads.

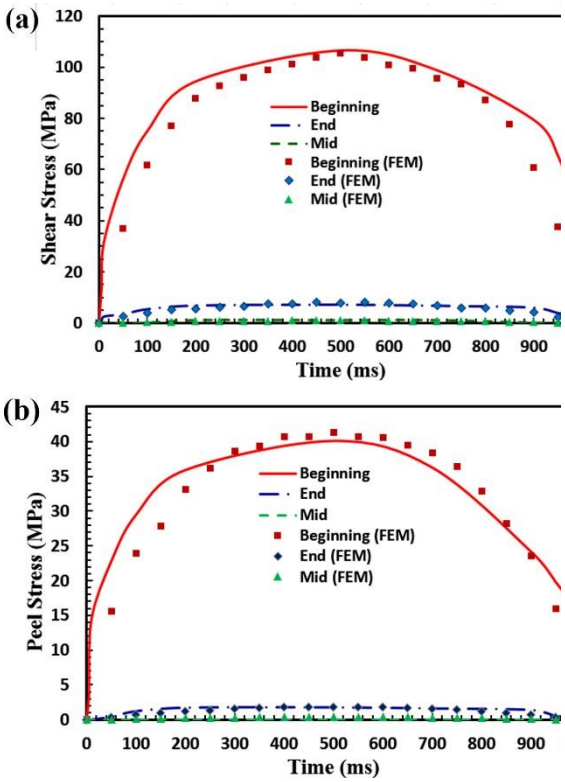

Fig. 8. Time variation diagrams of a) shear stress and b) peel stress in the adhesive layer of the bonded joint subjected to dynamic axial load

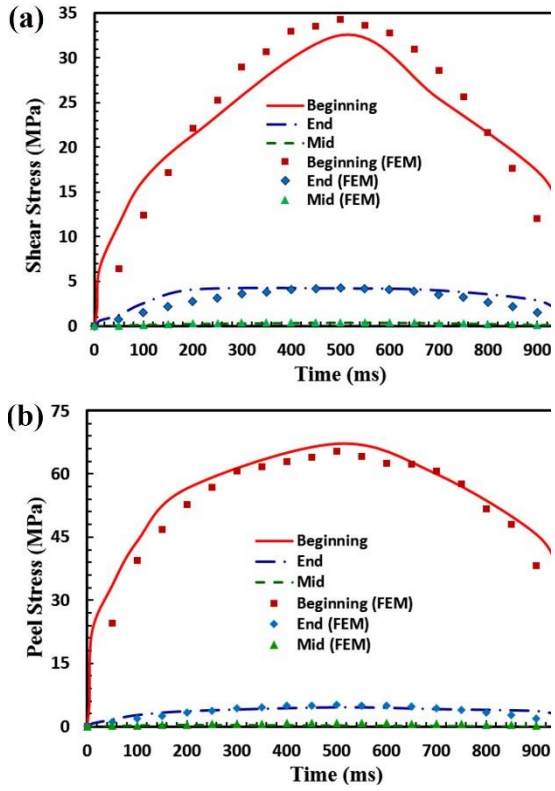

Fig. 9. Time variation diagrams of a) shear stress and b) peel stress in the adhesive layer of the bonded joint subjected to dynamic shear load

References

[1] Volkersen O. Nietkraftverteilung in ZugBeanspruchten niet ver Bindungen mit Konstanten Lashenquers Chnit-ten. *Luftfahrt Forschung* 1938; 15: 41-7.

[2] Goland M, Reissner E. The Stresses in Cemented Joints. J of Applied Me-chanics. *Journal of Applied Mechanics* 1994; 15: A17-A27.

[3] Hart-Smith LJ. Adhesive Bonded Scarf and Stepped Lap Joints. Douglas Aircraft Company, NASA,; 1973. Report No.: CR 112237.

[4] Hart-Smith LJ. Adhesive Bonded Single Lap Joints. Douglas Aircraft Company, NASA; 1973. Report No.: CR 112236.

[5] Hart-Smith LJ. Adhesive Bonded Double Lap joints. Douglas Aircraft Company, NASA; 1973. Report No.: CR 112235.

[6] Mortensen F, Thomsen OT. Analysis of Adhesive Bonded Joints: a Unified Approach. *Composites Science and Technology* 2002; 62: 1011- 32.

[7] Selahi E, Rajabi I, Behzadi M, Kadivar MH. Analysis of Adhesive Double Lap Joint for Com-posite Materials. In: Proceedings of the International Conference on Recent Advances in Composite Materials; 2004; Varanasi, India.

[8] Selahi E, Rajabi I, Jamali MJ, Kadivar MH. Analysis of Adhesive Double Strap Joint for Composite Materials. In: Proceedings of the international Conference on Recent Advances in Composite; 2004; Varanasi, India.

[9] Selahi E, Rajabi I, Kadivar MH. Mathematical Modeling of Composite Single Scarf Adhesive Joint. In: 13th. International Mechanical Engineering Conference, Isfahan, Iran; 2005.

[10] Selahi E, Tahani M, Yousefsani SA. Analytical Solutions of Stress Field in Adhe-sively Bonded Composite Single-lap Joints under Mechanical Loadings. *International Journal of Engineering* 2014; 27(3): 475- 6.

[11] Selahi E, Kadivar MH. Non-linear Analysis of Adhesive Joints in Com-posite Structures. *International Journal of Advanced Design and Manufacturing Technology* 2016; 9(1): 91-101.

[12] Selahi E. Elasticity Solution of Adhesive Tubular Joints in Laminated Composites, with Axial Symmetry. *Archive of Mechanical Engineering* 2018; LXV(3): 441- 56.

[13] Benchiha A, Madani K. Influence of the Presence of Defects on the Stresses Shear Distribution in the Adhesive Layer for the Single-lap Bonded Joint. *Structural Engineering and Mechanics* 2015; 53(5): 1017- 30.

[14] Radice J, Vinson J. On the Use of Quasi Dynamic Modeling for Com-posite Material Structures: Analysis of Adhesive-ly Bonded Joints with Midplane Asymmetry and Transverse Shear Deformation. *Composites Science and Technology* 2006; 66(14): 2528-47.
[15] Wu W, Liu Q, Zong Z, Sun G, Li Q. Experimental Investigation into Transverse Crashworthiness of CFRP Adhesively Bonded Joints in Vehicle Structure. *Composite Structures* 2013; 106: 581-9.
[16] Hazimeh R, Challita G, Khalil K, Othman R. Finite Element Analysis of Adhesively Bonded Composite Joints Subjected to Impact Loadings. *International Journal of Adhesion and Adhesives* 2015; 56: 24- 31.
[17] Araújo HAM, Machado JJM, Marques EAS, da Sil-va LFM. Dynamic Behaviour of Composite Adhesive Joints for the Automotive Industry. *Composite Structures* 2017; 171: 549- 61.
[18] He B, Ge D. Dynamic Strength of Adhesively Bonded Compo-site Joints with Similar and Dissimilar Assem-bled Adherends. *Journal of Reinforced Plastics and Composites* 2017; 36(23): 1683- 92.
[19] Argoud N, Rousseau J, Piezel B, Chettah A, Cadu T, Fiore A, et al. Multi-Axial Testing of Thick Adhesive Bonded Joints of Fibre Reinforced Thermoplastic Poly-mers. *International Journal of Adhesion and Adhesives* 2018; 84: 37- 47.
[20] Sassi S, Tarfaoui M, Benyahia H. An Investigation of In-plane Dynamic Behavior of Adhesively-Bonded Composite Joints under Dynamic Compression at High Strain Rate. *Composite Structures* 2018; 191: 168-79.
[21] Sassi S, Tarfaoui M, Benyahia H. Experimental Study of the Out-of-plane Dynamic Behaviour of Adhesively Bonded Composite Joints Using Split Hopkinson Pressure Bars. *Journal of Composite Materials* 2018.